RASĀYAN *J. Chem.*
Vol. 19 | No. 4 | 1967-1974 | October-December | 2026
ISSN: 0974-1496 | e-ISSN: 0976-0083 | CODEN: RJCABP
http://www.rasayanjournal.com
http://www.rasayanjournal.co.in

EFFICIENT CORROSION RESISTANCE OF MILD STEEL IN HYDROCHLORIC ACID BY A CARBOTHIOAMIDE-BASED PYRAZOLINE: ELECTROCHEMICAL, ADSORPTION AND DFT STUDIES

J. Kudva , P. Shekara✉, and P. R. D'Souza
Department of Chemistry, St Joseph Engineering College, 575028, (Karnataka), India.
✉Corresponding author: prathimas@sjec.ac.in

ABSTRACT
A newly synthesized carbothioamide-based pyrazoline was examined for its inhibition action against corrosion of mild steel in 0.5 M hydrochloric acid. Electrochemical techniques were employed to evaluate its performance. Results from electrochemical impedance spectroscopy (EIS) showed an inhibition efficiency of 81.27%. Potentiodynamic polarisation (PDP) studies yielded a similar result, with an efficiency of 82.28% at a 50 ppm concentration, confirming the good inhibitory action of CBP. The adsorption of CBP on the mild steel surface complied with the Langmuir adsorption isotherm. Quantum chemical calculations were carried out using Gaussian software. The UV-spectroscopic analysis confirmed the existence of a protective CBP film on the metal. The findings demonstrate that carbothioamide-based pyrazoline is a promising low-concentration corrosion inhibitor. This study supports the development of efficient corrosion mitigation strategies for industrial applications. The present work contributes to Sustainable Development Goal (SDG-9): Industry, Innovation and Infrastructure.
Keywords: Mild Steel, Pyrazolines, Electrochemical Techniques, Adsorption, Gaussian Software.
RASĀYAN *J. Chem.*, Vol. 19, No.4, 2026

INTRODUCTION

Mild steel is extensively used in industries because of its low cost, good mechanical strength, and ease of fabrication.[1] Its exposure to acidic media, like in acid pickling, cleaning, and descaling processes, causes severe corrosion. This leads to material degradation, economic losses, and safety concerns. Therefore, developing efficient corrosion protection strategies is essential for improving the durability of industrial infrastructure. [2] The organic inhibitors are considered one of the most effective and economical approaches. Compounds comprising heteroatoms such as nitrogen and sulfur, along with conjugated π-electron systems, adsorb on the metal.[3] So, heterocyclic compounds have received considerable attention as corrosion inhibitors.[4] Pyrazoline derivatives are attractive because of their electron-rich nitrogen atoms and aromatic framework. These structural features promote strong adsorption on the metal surface. Recent studies have shown that pyrazoline- and thiosemicarbazide-based compounds exhibit excellent corrosion inhibition in acidic media.[5] Their performance has been supported through electrochemical measurements and quantum chemical investigations. The studies on carbothioamide-based pyrazoline derivatives in 0.5 M HCl are still limited, and the reports combining electrochemical, adsorption, spectroscopic, and density functional theory (DFT) analyses are scarce.[6] Therefore, the present study investigates the anti-corrosive nature of a newly synthesized carbothioamide-based pyrazoline (CBP) for mild steel. Electrochemical impedance spectroscopy (EIS), potentiodynamic polarisation (PDP), adsorption studies, UV–Visible spectroscopy, and DFT calculations were employed to evaluate its inhibition efficiency. These techniques were also used to understand its adsorption behaviour and inhibition mechanism. The findings are anticipated to deliver useful insights into the design of efficient pyrazoline-based corrosion inhibitors for acidic industrial environments.

EXPERIMENTAL

Materials and Methods

The carbothioamide-based pyrazoline derivative CBP (Fig.-1) is synthesized and characterised as reported in our previous work.[7]

http://doi.org/10.31788/RJC.2026.1949996

Specimen Preparation
A commercial-grade mild steel (MS) specimen was cleaned, dried, and embedded in epoxy resin prior to electrochemical analysis.

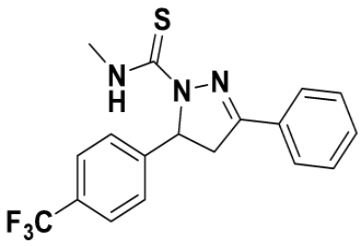

Fig.-1: Molecular Structure of CBP

Preparation of Corrosive Medium
The corrosive medium consisted of 0.5 M HCl containing CBP concentrations of 5, 20, 35, and 50 ppm. Fresh solutions were prepared prior to each experiment.

Techniques used in Electrochemical Measurement
Electrochemical tests employed a conventional cell of three electrodes (MS, Pt and SCE) connected to a CH608 E-series potentiostat. MS samples were soaked in 0.5 M HCl with 5, 20, 35, or 50 ppm CBP inhibitor concentration.

UV-Visible Spectroscopic Analysis
UV–Visible spectra were acquired using a UV-1900i spectrophotometer to examine the interaction between CBP and the mild steel surface.

Quantum Chemical Calculation
The quantification of quantum chemical parameters was executed at the DFT/B3LYP level with a 6-311++G (2d, p) basis set deployed in Gaussian 16 software. It relates inhibitor molecular structure to corrosion efficiency.[8,9]

RESULTS AND DISCUSSION

Electrochemical Impedance Measurements
The MS samples were submerged in a 0.5 M solution containing varied CBP levels. The experiments were conducted with a temperature variation from 303 to 323 K. EIS quantifications were then executed at OCP.[10] The obtained data were plotted in the form of Nyquist plots. In Nyquist analysis, R_p is estimated using the variance between high-frequency and low-frequency values.[11]An equivalent circuit model consisting of solution resistance (R_s) and polarisation resistance (R_p)was employed for inference of results (Fig.-2). It also consists of double-layer capacitance (C_{dl}).[12] It accounts for frequency dispersion in the system. It is described using a homogeneity parameter, denoted as (n).
The percentage corrosion inhibition efficiency (*% IE*) was computed employing the equation,

$$IE\ (\%) = \frac{R_p - R_p^0}{R_p} \times 100 \qquad (1)$$

C_{dl} is found with the following equation.

$$C_{dl} = \left[Y_0 R_{ct}^{(1-n)}\right]^{\frac{1}{n}} \qquad (2)$$

Where, Y_0 indicates the proportional factor (magnitude of CPE), R_{ct} indicates the resistance of charge transfer.[13]

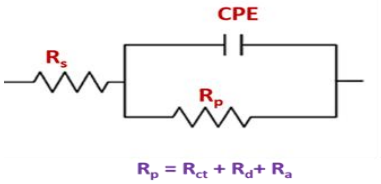

Fig.-2: (a) The Equivalent Circuit for all Nyquist Plot

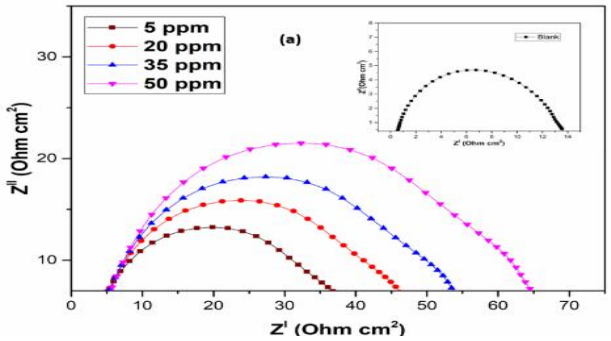

Fig.-3: Nyquist Plot of Various Concentrations of CBP in 0.5 M HCl at 303K.

The interpretation of impedance data was gauged using Nyquist plots (Fig.-3) with ZSimpWin software.[14] Table-1 shows that increasing CBP concentration increases R_p and decreases C_{dl}. Higher R_p indicates improved corrosion resistance due to inhibitor adsorption. Lower C_{dl} suggests reduced dielectric constant and increased double layer thickness.[15] These observations confirm the active adsorption of CBP on the metal surface, demonstrating its excellent corrosion inhibition performance in 0.5 M HCl. CBP showed an inhibition efficiency of 81.27% at 50 ppm of CBP concentration at 303 K. When the temperature was increased to 323 K in 0.5 M HCl, the efficiency decreased to 76.17%. This reduction is attributed to the detachment of CBP molecules at an elevated temperature from the metal surface.[16]

Table-1: Impedance Data of Mild Steel with and without CBP

Temp.(K)	Conc. (ppm)	R_s (Ohm cm^2)	R_p (Ohm cm^2)	C_{dl} (µF)	n	IE (%)
303	Blank	2.90	11.26	110.26	0.85	
	5	2.103	37.15	28.26	0.77	69.69
	20	1.862	42.44	17.00	0.79	73.47
	35	1.783	50.31	14.84	0.77	77.62
	50	1.785	60.12	11.35	0.75	81.27
313	Blank	2.79	9.40	141.51	0.84	
	5	2.03	28.49	51.31	0.81	67.01
	20	1.88	31.35	34.74	0.81	70.02
	35	1.828	37.98	28.45	0.80	75.25
	50	1.886	44.61	14.42	0.80	78.93
323	Blank	2.62	7.96	178.74	0.86	
	5	2.251	22.55	89.64	0.82	64.70
	20	2.813	25.06	61.16	0.81	68.23
	35	1.877	28.40	44.54	0.79	71.97
	50	1.633	33.40	20.19	0.73	76.17

Potentiodynamic Polarisation Measurements

Figure-4 indicates the curves for mild steel generated by potentiodynamic polarisation in 0.5 M HCl. The corresponding data are listed in Table-2. The cathodic branches are not exactly parallel, unlike the anodic slopes. This indicates that CBP influences the cathodic reaction. The rate (CR) and density (i_{corr}) of corrosion decline with increasing CBP concentration, which proves that the inhibitor blocks active sites and consequently reduces the corrosion process.[17]

A larger change in the anodic Tafel slope suggests dominant anodic inhibition. A negative shift in the corrosion potential (E_{corr}) was observed with increasing CBP concentration, with a maximum displacement of approximately 65 mV relative to the blank solution. Since the shift remained below 85 mV, CBP serves as a mixed-type inhibitor by retarding both iron dissolution and the hydrogen evolution reaction. The simultaneous decline in the anodic and cathodic Tafel slopes further supports this behaviour, indicating that the adsorbed CBP molecules effectively suppress both electrode reactions in the acidic medium.[18]

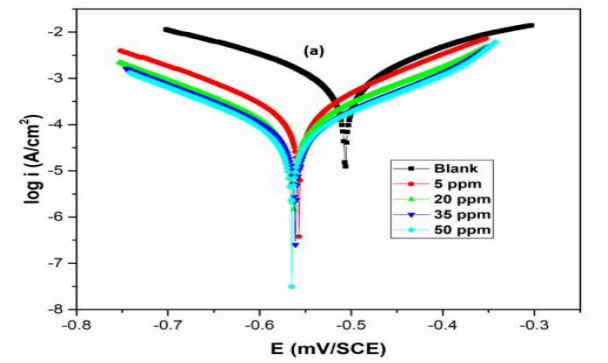

Fig.-4: Tafel Curves Mild Steel Corrosion in 0.5 M HCl on Variation of CBP Concentrations at 303 K

Table-2: PDP Data of Mild Steel Corrosion using CBP Concentration Variation in 0.5 M HCl.

Temp. (K)	Conc. (ppm)	$-E_{corr}$ (mV)	$-\beta_c$ (mV)	β_a (mV)	i_{corr} ($\mu A\ cm^{-2}$)	CR (mmy^{-1})	IE (%)
303	Blank	0.511	158.73	147.06	2244	26.028	
	5	0.520	130.11	114.44	600	6.959	73.10
	20	0.529	125.08	109.21	530	6.148	76.42
	35	0.513	132.52	123.33	460	5.336	79.30
	50	0.531	125.20	125.93	400	4.640	82.28
313	Blank	0.501	151.26	165.59	2560	32.675	
	5	0.513	127.65	113.05	830	9.627	70.71
	20	0.563	127.81	114.10	760	8.815	73.00
	35	0.57	127.81	121.61	660	7.655	76.68
	50	0.484	124.27	122.04	600	6.959	78.97
323	Blank	0.484	154.15	173.55	3281	38.057	
	5	0.522	134.03	118.16	1050	12.179	68.12
	20	0.514	137.72	134.35	980	11.367	70.25
	35	0.531	141.78	124.30	920	10.671	71.95
	50	0.523	155.69	130.28	850	9.859	74.12

The corrosion current density (i_{corr}) decreased to 400, 600, and 850 μAcm^{-2} at 303, 313, and 323 K, respectively, in the presence of 50 ppm CBP in 0.5 M HCl. The maximum inhibition capability of 82.28% was obtained at 303 K, which is in good agreement with the value derived from EIS measurements. These results confirm the adsorption of CBP onto the MS, forming a protective barrier against corrosion.[19]

Adsorption Considerations

Adsorption isotherms are essential for interpreting the adsorption behaviour of inhibitors on MS. Among the different models tested, only the Langmuir isotherm showed a regression coefficient close to unity. The good linearity of the Langmuir plot (Fig.-5) indicates monolayer adsorption of CBP on energetically uniform active sites of the mild steel surface.[20]

Table-3: Adsorption Parameters for CBP

Temp.(K)	R^2	K	ΔG
303	0.999	65547.98	-38.03
313	0.999	63411.54	-39.20
323	0.999	82372.32	-41.16

Langmuir isotherm was applied using surface coverage (θ) values from PDP measurements.[21]

$$\frac{C}{\theta} = \frac{1}{K_{ads}} + C \quad (3)$$

The negative value of $\Delta G°_{ads}$ (around −40 kJ/mol) in Table-3 suggests that the inhibition process by CBP involves both physical and chemisorptive interactions between the inhibitor molecules and the metal surface.

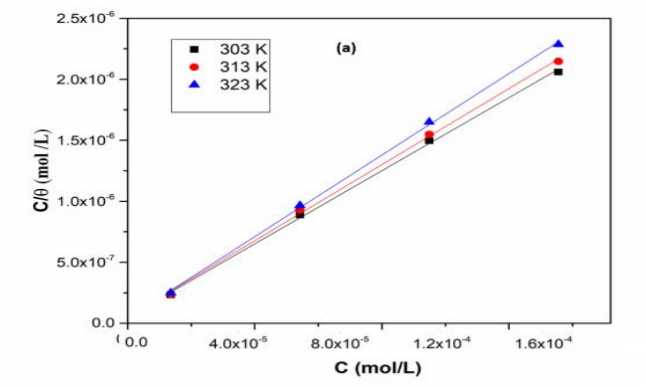

Fig.-5: Langmuir Adsorption Isotherm Obtained for CBP

UV-Visible Spectroscopic Analysis

Spectrum of the CBP (Fig.-6) shows two distinct peaks at 320 nm, exhibiting the absorbance value of 1.219, and at 261 nm, exhibiting the absorbance value of 1.44. The spectrum of the inhibitor solution after mild steel immersion exhibited one sharp peak at 255 nm with the increase in absorbance value (1.87), whereas the peak at a higher wavelength was almost vanished. The changes in absorbance and the slight shift in the absorption band after exposure of the mild steel coupon indicate the interaction of CBP molecules with iron ions released from the metal surface.[22] Such spectral changes suggest the formation of an adsorbed inhibitor–metal complex.[23]

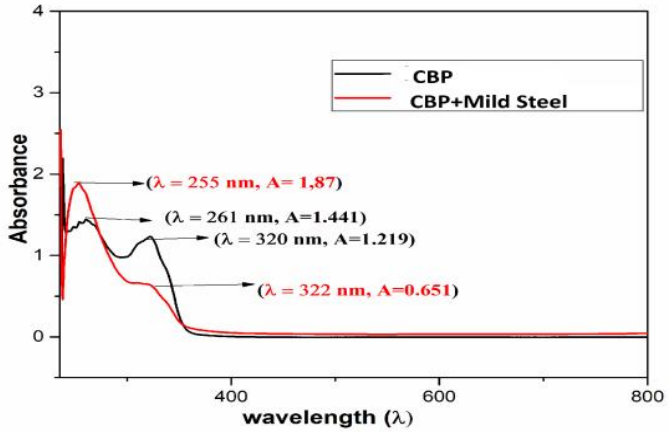

Fig.-6: UV -Spectra of CBP before and after Immersion of Mild Steel.

Theoretical Quantum Chemical Calculation

DFT calculations were carried out to better understand the adsorption behaviour of CBP on the mild steel surface.[24] The chemical calculations were performed, followed by evaluation of key descriptors, including E_{HOMO}, E_{LUMO}, energy gap (ΔE), fraction of electron transfer (ΔN), dipole moment (μ), global softness (S), and hardness (η), as derived from Koopmans' theorem and summarised in Table-4.

The optimised geometries and frontier molecular orbital distributions of CBP a are shown in Fig.-7. Both HOMO and LUMO densities are localised on the pyrazoline ring and C=S group of the methyl thio semicarbazide moiety. These features suggest involvement of multiple functional groups in donor–acceptor electronic interactions.[25]

Table-4: Quantum Chemical Parameters for CBP.

Parameters(B3LYP method)	CBP in aqueous phase(eV)
Energy of HOMO	-6.039
Energy of LUMO	-1.707
ΔE	4.332
$-E_{HOMO}$ (I)	6.039
$-E_{LUMO}$ (A)	1.707
Electrophilicity (ω)	19.962
Electronegativity(χ)	3.873
Hardness (η)	2.166
Softness (s)	0.461
Dipole moment μ (debye)	9.3
ΔN (Fractions of electrons transferred)	0.721

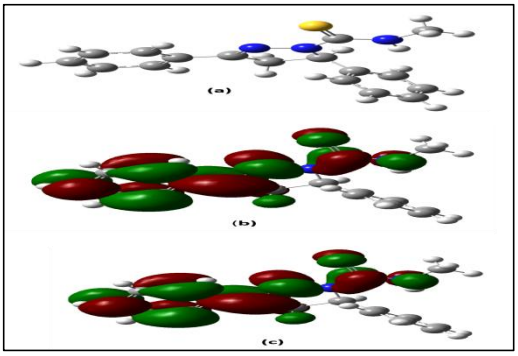

Fig.-7: Structure of CBP (a) Optimised, (b) HOMO, and (c) LUMO

It is observed that CBP exhibits a smaller energy gap (ΔE = 4.332 eV). This indicates stronger electron-donating ability and greater inhibitor efficiency. The lower electronegativity supports enhanced electron donation to the metal surface. According to the HSAB principle, mild steel acts as a soft acid, favouring interactions with soft base molecules. CBP shows higher softness (S = 0.461 eV). This proves stronger soft–soft interactions. The fraction of electrons transferred (ΔN) was also higher (0.721). These observations highlight a greater tendency of CBP to donate charge. The dipole moment is an indication that can be used to predict how a corrosion inhibition procedure will proceed.[26]

Mechanism of Inhibition

In the present study, carbothioamide-based pyrazoline derivatives exhibited exceptional corrosion resistance, supported by both experimental data and theoretical modelling. In 0.5 M HCl, CBP molecules are expected to exist in both neutral and protonated forms. These species adsorb on the MS surface through electrostatic interactions between the electron-rich nitrogen and sulfur atoms and the unfilled orbitals of iron.[27] Once anchored to the surface, the inhibitors interact with Fe^{2+} ions generated during the corrosion process, forming stable metal–inhibitor complexes. The protonated inhibitor species can electrostatically bind to pre-adsorbed chloride ions, promoting physisorption. The electron-rich nitrogen and sulfur atoms, along with the aromatic π-electron system, readily interact with the vacant d-orbitals of iron. This interaction promotes the formation of coordination bonds, resulting in a stable protective film that minimises corrosion.

CONCLUSION

In conclusion, the new pyrazoline derivative, namely CBP, was synthesised successfully and characterised using spectroscopic techniques. Electrochemical tests identified CBP as a mixed-type inhibitor, where CBP minimises both cathodic hydrogen evolution and anodic dissolution of mild steel. The CBP molecules complied with the Langmuir isotherm model in the adsorption process. Thermodynamic evaluations confirmed that the adsorption is spontaneous and follows chemisorption as a predominant process. The UV–visible techniques affirmed the generation of a protective film of the CBP on the mild steel surface, with the Quantum chemical simulations revealing a small HOMO–LUMO

energy gap and a high electron transfer fraction, indicating the strong anticorrosion capability of carbothioamide-based structures. At a low dosage of 50 ppm, the synthesised inhibitors exhibited remarkable inhibition efficiency at low temperature. The effective corrosion inhibition demonstrated by CBP contributes to improving the durability of metallic infrastructure supporting Sustainable Development Goal (SDG-9).

CONFLICT OF INTERESTS

The authors declare no potential conflicting interests.

AUTHOR CONTRIBUTIONS

The present work is related to *SDG-9: Industry, Innovation and Infrastructure*. All the authors contributed significantly to this manuscript, participated in reviewing/editing and approved the final draft for publication. The research profile of the authors can be verified from their ORCID ids, given below:

Jyothi Kudva https://orcid.org/0000-0002-2055-4460
Prathima Shekara https://orcid.org/0009-0005-7260-2857
Pramila Rita D'Souza https://orcid.org/0000-0002-8575-5706

Cite this article as: P. R. Dsouza *et al.*, *Rasayan J. Chem.*, 19(4), 1967-1974(2026), https://doi.org/10.31788/RJC.2026.1949996

REFERENCES

1. F. Hashim, K.F.A. Hazavi, A. Amiery, *Proceedings,* **41**, 1(2019).
2. H.R. Raveesha, *Journal of Science of Advanced Materials and Devices,* **4**, 57(2019), https://doi.org/10.1016/j.jsamd.2019.01.003.
3. D. Patil, U.P. Lad, R. S Patil J. U. Patil O. S. Kushwaha and T. J. Shinde, *Rasayan. Journal of Chemistry,* **19**, 3(2026) , https://doi.org/10.31788/RJC.2026.1939283.
4. G.H. Sayed, M.E. Azab, K.E. Anwer, M.A. Raouf, and N. A. Negm, *Journal of Molecular Liquids,* **252**, 134(2018), https://doi.org/10.1016/j.molliq.2017.12.156
5. A.B. Kamal, M.A. Mostfa, A.M. Ashmavy, M.S.A Elgaby and G.A. Ali, *Journal of Chemical Sciences,* **134,** 90(2022), https://doi.org/10.1007/s12039-022-02086-6.
6. T.C. Leboho, K. Selowa, R.K.Mothapo, T.Pesha, B.P. Moloto, *Results in Surfaces and Interfaces,* **23**, 100778(2026), https://doi.org/10.1016/j.rsurfi.2026.100778.
7. P. Shekara, J. Kudva, R. Sadashiva, D. Naral, and A.N. Shetty, *Chemical Data Collections*, **37**, 100808(2022), https://doi.org/10.1016/j.cdc.2021.100808.
8. A. Elbarki, *Chemical Data Collections*, **28**, 100454(2020), https://doi.org/10.1016/j.cdc.2020.100454.
9. A. Ziouani, S. Atia, H. Hamani, T. Douadi, M. Al-Noaimi, N. Gherraf, *Journal of Indian Chemical Society*, **100**, 100832(2023), https://doi.org/10.1016/j.jics.2022.100832.
10. A.K. Singh, S. K. Shukla, M.A. Quraishi, E.E. Ebenso, *Journal of the Taiwan Institute of Chemical Engineers,* **43**, 463(2012), https://doi.org/10.1016/J.JTICE.2011.10.012.
11. A.S. Fouda, F.E. Heakal, M. S. Radwan, *Journal of Applied Electrochemistry*, **39**, 391(2009), https://doi.org/10.1007/s10800-008-9684-2.
12. M. Prabakaran, K. Vadivu, S. Ramesh, and V. Periasamy, *Journal of Materials and Environmental Science*, **5**, 553(2014).
13. Z. Mahidashti, T. Shahrabi, and B. Ramezanzadeh, *Progress in Organic Coatings,* **114**, 19(2018), https://doi.org/10.1016/j.porgcoat.2017.09.015.
14. A. Masoumi, M.H. Sadr, and B. Soltani, *Journal of Adhesion Science and Technology*, **34**, 2569(2020), https://doi.org/10.1080/01694243.2020.1771973.
15. M.A. Abbas, A.M. Eid, M.M. Abdou, A. Elgendy, R. A. El-Saeed, E. G. Zaki, *ACS Omega*, **6**, 8894(2021), https://doi.org/10.1021/acsomega.0c06050.
16. L.P. Chaudhari and S.N. Patel, *Journal of Bio and Tribo-Corrosion*, **5**, 1(2019),

https://doi.org/10.1007/s40735-018-0212-6.
17. M.A. Amin, K.F. Khaled, S.A. Fadl-Allah, *Corrosion Science,* **52**, 14(2010), https://doi.org/10.1016/j.corsci.2009.08.055.
18. A. Sehmi, H.B. Ouici, A. Guendouzi, M. Ferhat, O. Benali, F. Boudjellal, *Journal of The Electrochemical Society*, **167**, 155508(2020), https://doi.org/10.1149/1945-7111/abab25.
19. S. John, A. Joseph, A.J. Jose, B. Narayana, *Progress in Organic Coatings*, **84**, 28(2015), https://doi.org/10.1016/j.porgcoat.2015.02.005.
20. K.V. Shenoy, P.P. Venugopal, P.D.R. Kumari, D. Chakraborty, *Journal of Molecular Structure,* **1232**, 130074(2021), https://doi.org/10.1016/j.molstruc.2021.130074.
21. H. Lgaz, R. Salghi, A. Chaouiki, Shubhalaxmi, S. Jodeh, K. Subrahmanya Bhat, *Cogent Engineering,* **5**, 1441585(2018), https://doi.org/10.1080/23311916.2018.1441585.
22. E.E. El-katori, R.A. El-saeed, M.M. Abdou, *Arabian Journal of Chemistry,* **15**, 104373(2022), https://doi.org/10.1016/j.arabjc.2022.104373.
23. A.M. Ashmawy, M.A. Mostafa, A.B. Kamal, G.A.M. Ali, M. S.A. El-Gaby, *Scientific Reports,* **13**, 18555(2023), https://doi.org/10.1038/s41598-023-45659-2.
24. S. Chen, B. He, Y. Liu, Y. Wang, J. Zhu, *International Journal of Electrochemical Science,* **9,** 5400(2014), https://doi.org/10.1016/S1452-3981(23)08176-2
25. N.O. Eddy, H.M. Hayaya, E.E. Oguizi, *Journal of Advanced Research*, **6**, 203(2015), https://doi.org/10.1016/j.jare.2014.01.004
26. I. Lukovits, E. Kálmán, and F. Zucchi, *Corrosion*, **57**, 3(2001), https://doi.org/10.5006/1.3290328.
27. F. Iorhuna, A.S. Muhammad, A.M. Ayuba, *Advanced Journal of Chemistry-Section A*, **6**, 71(2023), https://doi.org/10.22034/AJCA.2023.370123.1347

[RJC-9996/2026]